In-Plane Seismic Behavior of Rectangular Steel-Plate Composite Wall Piers

Siamak Epackachi, A.M.ASCE[1]; Nam H. Nguyen[2]; Efe G. Kurt[3]; Andrew S. Whittaker, M.ASCE[4]; and Amit H. Varma, M.ASCE[5]

Abstract: An experimental study investigated the behavior of large-scale steel-plate composite (SC) walls subjected to cyclic lateral loading. The testing program involved four rectangular SC wall specimens with an aspect ratio (height-to-length) of 1.0. The specimens were anchored to a concrete basemat with a pretensioned bolted connection that was designed to be stronger than the walls. The design parameters considered in the investigation were wall thickness, reinforcement ratio, stud spacing, and tie bar spacing. The pretest analyses, global force-displacement responses, contributions of the steel faceplates and infill concrete to the lateral resistance, load transfer between the faceplates and infill concrete, and damage to the face plates and infill, are documented. The four SC walls failed in a flexural mode characterized by tensile cracking of the concrete, tensile yielding of the steel plates, crushing of concrete at the toes of the wall, outward local buckling of the steel faceplates, and fracture of the steel faceplates. The walls achieved the peak shearing strengths estimated using simplified procedures and ABAQUS. Pinching of the force-displacement response was observed at displacements greater than those associated with peak load. The distance between the baseplate and the first row of connectors affected the postpeak shear strength behavior and the fracture of the faceplates. The connection of the SC wall to the foundation block had a significant influence on the initial stiffness of the walls. **DOI: 10.1061/(ASCE)ST.1943-541X.0001148.**

Author keywords: Steel-plate composite shear wall; Safety-related nuclear structure; Flexure-critical wall; Cyclic loading; Hysteresis loops; Metal and composite structures.

Introduction and Background

Steel-plate composite (SC) walls, consisting of steel faceplates, infill concrete, headed steel studs anchoring the faceplates to the infill, and tie rods connecting the two faceplates through the infill, have potential advantages over conventional reinforced concrete walls due to their relatively high shear strength, deformation capacity, and ease of construction. To date, design of SC walls has been based in part on proprietary test data and limited data available in the literature. Most of these tests were conducted at small scales and have focused on the *essentially elastic* range of response.

Although SC wall construction is not new, it has yet to see widespread use in the building industry. In the last four decades, a number of research projects have investigated the performance of SC walls for use in tunnels, blast resistant shelters, and liquid and gas retaining structures. The use of SC wall construction in nuclear power plants has been studied for nearly 20 years, with an emphasis on elastic response in design basis shaking. Application of SC walls to containment internal structures and shield buildings in nuclear power plants has begun in the United States and China (e.g., Varma et al. 2014; Zhang et al. 2014).

The use of ice-resisting SC walls for offshore construction was proposed in the late 1970s by the Hitachi Shipbuilding and Engineering Company (Adams et al. 1987), which prompted further studies (e.g., Gerwick and Dale 1987; Matsuishi and Iwata 1987; O'Flynn and MacGregor 1987; Smith and McLeish 1987; Link and Elwi 1995). Double skin composite construction was proposed in 1987 for submerged tunnels. Pilot tests were performed and design guidelines were drafted by Wright and his coworkers (e.g., Oduyemi and Wright 1989; Wright et al. 1991a, b).

The use of SC walls in safety-related nuclear structures in Korea, Japan, and the United States has been studied for the past 20 years. Small-scale tests were performed to develop a body of data on the in-plane shear, out-of-plane shear, and thermal performance of SC walls for different reinforcement ratios and concrete strengths (e.g., Akiyama et al. 1989; Sasaki et al. 1995; Takeda et al. 1995; Takeuchi et al. 1995; Usami et al. 1995; Akita et al. 2001; Kazuaki et al. 2001; Ozaki et al. 2001, 2004). The Japanese data were used to develop the Japanese code on SC wall construction: JEAG 4618 (JEA 2005). Korean researchers followed the Japanese lead and conducted companion experiments, also at a small scale. The proprietary Korean data were used to aid the design of the APR 1400+ power plant and the development of the Korean code for design of SC walls in nuclear facilities. A design code for SC walls in nuclear structures is currently in preparation in the United States: AISC N690s1 (2014). This draft standard under public review is based on recent tests performed in the United States (e.g., Booth et al. 2007; Sener and Varma 2014; Varma et al. 2011, 2012, 2013, 2014), available Korean and Japanese data,

[1]Ph.D. Candidate, Dept. of Civil, Structural and Environmental Engineering, Univ. at Buffalo, Buffalo, NY 14260 (corresponding author). E-mail: siamakep@buffalo.edu

[2]Ph.D. Candidate, Dept. of Civil, Structural and Environmental Engineering, Univ. at Buffalo, Buffalo, NY 14260. E-mail: namnguye@buffalo.edu

[3]Ph.D. Candidate, School of Civil Engineering, Purdue Univ., West Lafayette, IN 47907. E-mail: ekurt@purdue.edu

[4]Professor and Chair, Director, MCEER, Dept. of Civil, Structural and Environmental Engineering, Univ. at Buffalo, Buffalo, NY 14260. E-mail: awhittak@buffalo.edu

[5]Professor, School of Civil Engineering, Purdue Univ., West Lafayette, IN 47907. E-mail: ahvarma@purdue.edu

Note. This manuscript was submitted on November 6, 2013; approved on June 26, 2014; published online on August 14, 2014. Discussion period open until January 14, 2015; separate discussions must be submitted for individual papers. This paper is part of the ***Journal of Structural Engineering***, © ASCE, ISSN 0733-9445/04014176(9)/$25.00.

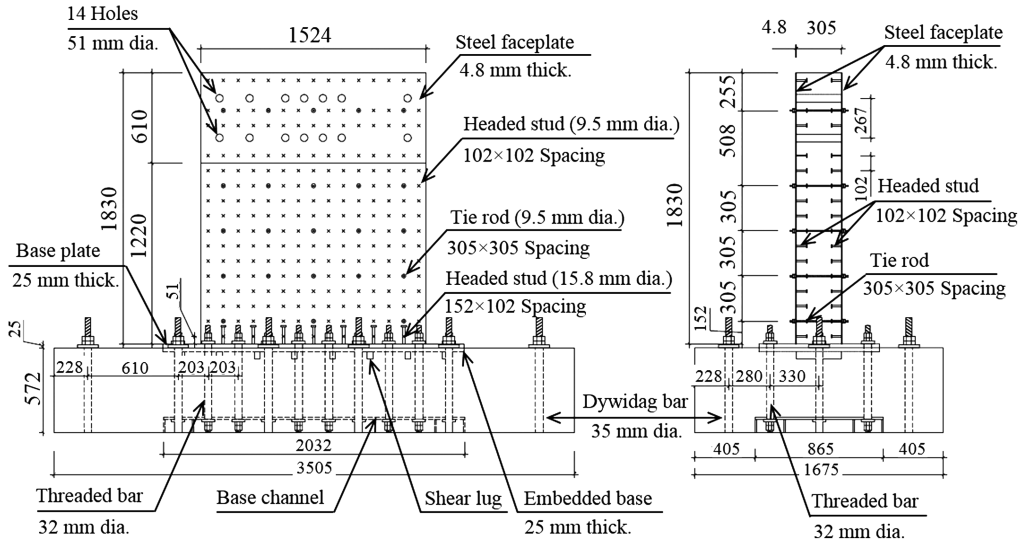

Fig. 1. Elevation view and cross section through specimen SC1

and the results of numerical simulations performed by Varma and his coworkers (Varma et al. 2013, 2014; Zhang et al. 2014).

Walls in safety-related nuclear facilities are typically constructed with flanges (cross walls) or boundary elements, forming I-shaped or rectangular cross sections. Walls in buildings may either be rectangular or constructed with flanges or boundary elements. The lateral load response of SC walls with large flanges or boundary elements is typically governed by the in-plane shear response of the web of the wall (Ozaki et al. 2004; Varma et al. 2011, 2014) whereas the response of rectangular SC walls (also known as wall piers) is a function of combined in-plane flexure and in-plane shear, with the relative contributions dictated by aspect ratio.

This paper addresses the inelastic cyclic lateral load response of four rectangular, flexure-critical SC walls. Only in-plane loading was considered. Although many large-scale tests will have to be undertaken to fully understand the seismic response of SC walls through failure under in-plane and out-of-plane loadings, these four tests enable the validation of numerical models and tools for the purpose of design and assessment. The following sections of the paper describe the testing program and pretest analyses and present key experimental results and conclusions. The numerical models developed for finite element analysis of SC walls and the macro-models developed for analysis of structures incorporating SC walls are described elsewhere (e.g., Epackachi 2014).

Experimental Program

Test Specimen Description

Four large-size specimens (SC1 through SC4) were constructed and tested under displacement-controlled cyclic loading in the NEES laboratory at the University at Buffalo, with support from Bowen Laboratory at Purdue University. The aspect ratio (height-to-length, H/L) of all four walls was 1.0.

Each SC wall was installed on top of a reusable foundation block. The base of each wall included a 25.4-mm (1-in.) thick A572 Gr.50 steel base plate to which the faceplates were complete joint penetration (CJP) groove welded. Two rows of fifteen 15.8-mm (0.675-in.) diameter headed steel studs were welded to the base plate to anchor the concrete and improve the transfer of shearing and tensile forces. The SC wall was anchored to the foundation block using twenty-two 32-mm (1.25-in.) diameter threaded B7 bars that were posttensioned to 445 kN (100 kips) per bar. Fig. 1 shows the elevation and cross-section views of specimen SC1. The anchorage to the foundation block was designed to be stronger than the corresponding SC wall specimens. The foundation block was effectively rigid.

Table 1 provides material and geometric information on the four walls. In this table, the studs and tie rods are spaced at distance S, the overall thickness of the wall is T, the thickness of each faceplate is t_p, the reinforcement ratio is $2t_p/T$, the faceplate slenderness ratio is S/t_p, and concrete strength (f'_c) is measured on the day of the tests. The diameters of the studs and tie rods were 9.5 mm (0.375 in.) for all walls.

Material Properties

The studs and tie rods were fabricated from carbon steel with a nominal yield strength of 345 MPa (50 ksi). The yield and ultimate strengths of the steel faceplates, calculated from three coupon tests, were 262 and 380 MPa (38 and 55 ksi), respectively. The nominal compressive strengths of the infill concrete and the foundation concrete were 27.5 and 42 MPa (4 and 6 ksi), respectively.

Table 1. Test Specimen Configurations

Specimen	Wall dimension ($H \times L \times T$) [mm × mm × mm (in. × in. × in.)]	Stud spacing [mm (in.)]	Tie rod spacing [mm (in.)]	Reinforcement ratio (%)	Faceplate slenderness ratio	Day-of-test wall concrete strength [MPa (ksi)]
SC1	1,524 × 1,524 × 305 (60 × 60 × 12)	102 (4)	305 (12)	3.1	21	31.0 (4.5)
SC2	1,524 × 1,524 × 305 (60 × 60 × 12)	—	152 (6)	3.1	32	31.0 (4.5)
SC3	1,524 × 1,524 × 228 (60 × 60 × 9)	114 (4.5)	228 (9)	4.2	24	36.5 (5.3)
SC4	1,524 × 1,524 × 228 (60 × 60 × 9)	—	114 (4.5)	4.2	24	36.5 (5.3)

Design Variables

Reinforcement ratio is a key parameter for the design of SC composite walls, where the reinforcement ratio is defined as the ratio of the area of the faceplates divided by the total area of the SC wall web. Table 1 lists the reinforcement ratios for the specimens. Out-of-plane buckling of the steel faceplates and the load transfer between the steel faceplates and the infill concrete is influenced by the spacing of the connectors and so faceplate slenderness ratio, the ratio of the greatest spacing of the connectors (studs or tie rods) to the steel faceplate thickness, is another key design parameter. Based on the research of Zhang et al. (2014), AISC N690s1 (AISC 2014) specifies a maximum slenderness ratio to prevent faceplate buckling prior to yielding

$$\lambda_p = 1.0\sqrt{\frac{E_s}{f_y}} \tag{1}$$

where E_s and f_y = Young's modulus and nominal yield strength of the steel faceplate, respectively. For a yield strength of 262 MPa (38 ksi), the limiting slenderness ratio is 28. The values of the slenderness ratio listed in Table 1 indicate that SC1, SC3, and SC4 complied with this limit.

Pretest Analysis

Pretest analyses of trial SC walls were performed to inform the design, detailing, and instrumentation of the test specimens, design the reusable foundation block, and develop a loading protocol. Only those pretest calculations relevant to SC1 through SC4 are presented below.

Calculations were first performed to determine whether the specimens were flexure critical or shear critical and to establish the likely peak shearing strength. Nominal material properties were used. The flexural strengths of the SC walls were estimated using the cross-section program XTRACT (Chadwell and Imbsen 2002); the corresponding maximum shearing forces were 1,530 kNg (344 kips) and 1,460 kN (328 kips) for SC1/SC2 and SC3/SC4, respectively. The flexural strength calculation assumed a perfect bond between the steel faceplates and the infill concrete. The maximum shearing force based on the plastic moment in the faceplates alone was 1,378 kN (310 kips): 90 and 95% of the XRACT-based predictions for SC1/SC2 and SC3/SC4, respectively. The maximum shearing resistance of the walls per AISC N690s1 (AISC 2014), Ozaki et al. (2004), and Varma et al. (2011, 2012) was 3,870/3,800/3,625 kN (870/855/815 kips) for SC1/SC2 and 3,740/3,800/3,470 kN (840/855/780 kips) for SC3/SC4, which assumes shear yielding of the faceplates. These calculations showed the walls to be flexure critical, with a maximum resistance less than the capacity of the actuators proposed for loading the walls.

The general purpose finite element code ABAQUS (SIMULIA 2012a, b) was used to confirm the peak shearing strengths predicted by XTRACT and to predict the shearing force-lateral displacement relationships of the four walls. For the ABAQUS simulations, the concrete damage plasticity (CDP) model was used for the infill concrete and the J2 plasticity model with isotropic hardening was used for the steel faceplates. Friction between the infill concrete and the steel faceplates and buckling of the steel faceplates were considered. Beam elements were used to represent the studs and tie rods. Solid elements were used to model the infill concrete, foundation block, base plates, loading plates and posttensioning bars. Shell elements were used for the steel faceplates. The infill concrete was modeled with 25.4 × 25.4 × 25.4 mm (1 × 1 × 1 in.) elements and the steel faceplates were modeled with 12.7 × 12.7 mm (0.5 × 0.5 in.) elements. The model took advantage of symmetry to reduce the computational effort. The ABAQUS model is shown in Fig. 2. The ABAQUS-predicted

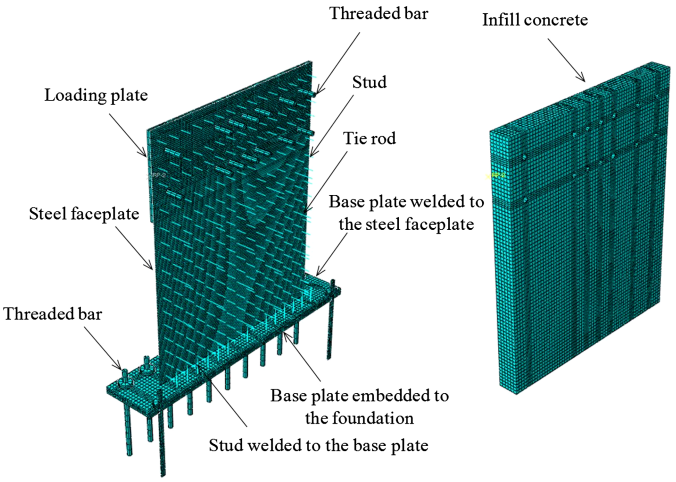

Fig. 2. ABAQUS modeling of SC1

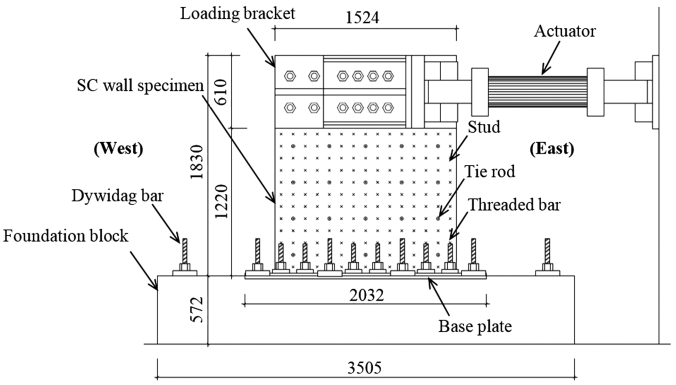

Fig. 3. SC wall test setup

maximum shearing forces were 1,312/1,423/1,156/1,267 kN (295/320/260/285 kips) for SC1 through SC4, respectively. The shearing forces corresponding to the flexural strengths estimated by XTRACT, which ignores flexure-shear interaction, agree reasonably well with peak shearing strengths predicted by ABAQUS.

Test Setup

Fig. 3 presents the test setup. Two horizontally inclined, high force-capacity actuators were used to apply quasistatic cyclic lateral loads

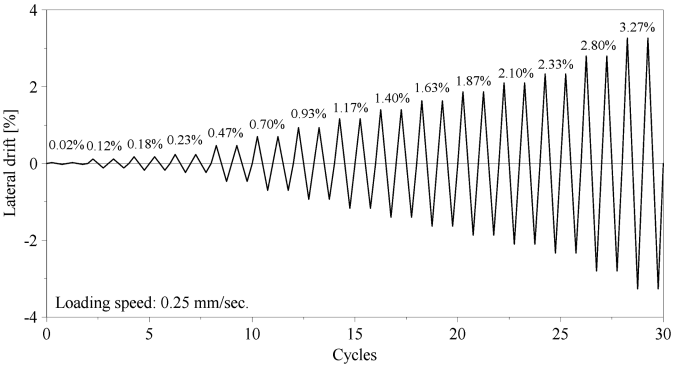

Fig. 4. Deformation history for SC walls

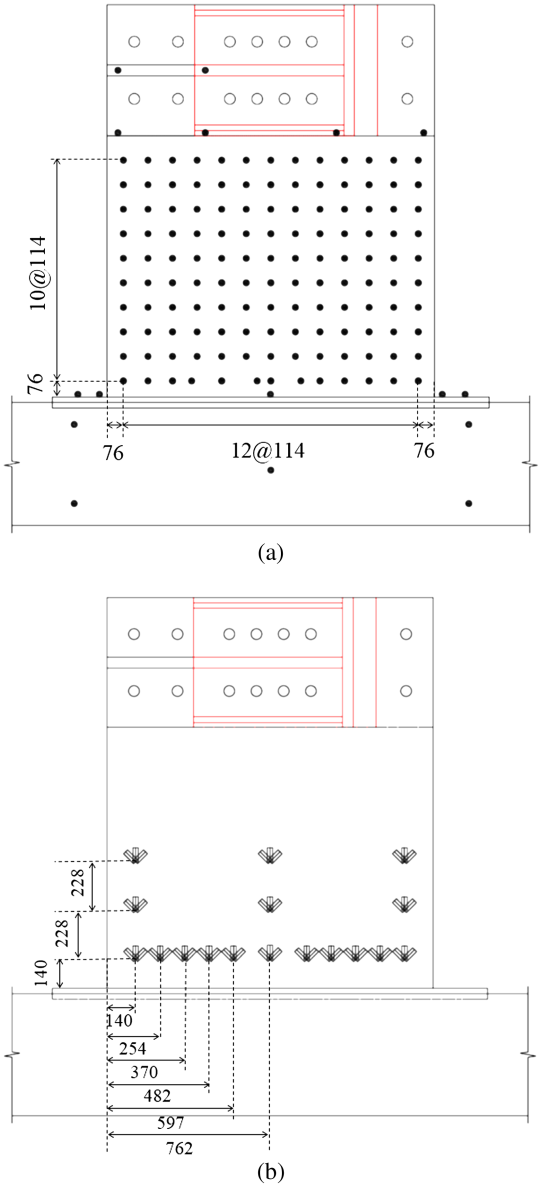

Fig. 5. Krypton LEDs and strain gauges on SC3: (a) Krypton LEDs; (b) Rosette strain gauges

at the top of the SC walls via loading brackets. The foundation block was posttensioned to the strong floor with fourteen 35-mm (1.5-in.) diameter Dywidag bars to prevent foundation movement during testing. The loading plates were attached to each specimen using fourteen 32-mm (1.25-in.) diameter B-7 threaded rods that were posttensioned to 445 kN (100 kips) per bar.

The displacement-controlled, reversed cyclic loading protocol was based on the recommendations of ACI 374.1-05 (ACI 2005). Two cycles of loading, with a speed of 0.25 mm/s (0.01 in./s), were imposed at displacements equal to fractions and multiples of a reference displacement [= 3.60 mm (= 0.14 in.)]: 0.1, 0.5, 0.75, 1, 2, . . . , 15, where the calculation of the reference displacement is described in Epackachi (2014). In each loading cycle, a push was exerted first, followed by a pull, where the push was defined as the loading in the positive direction to the west (denoted as WL+) and the pull was defined as the loading in the negative direction to the east (denoted as EL−). Testing was terminated after significant damage due to steel faceplate fracture and crushing of infill concrete at the toes of the walls. The loading protocol is presented in Fig. 4.

Instrumentation

Krypton light-emitting diodes (LEDs), rosette strain gauges, linear potentiometers, Temposonic displacement transducers, and linear variable displacement transducers were used to monitor the response of the walls. Potentiometers and Temposonics were attached to the ends of the walls to measure in-plane displacement. Four potentiometers attached to the corners of one steel faceplate measured the out-of-plane displacement of the walls. The movement of the foundation block relative to the strong floor was monitored using potentiometers and Krypton LEDs.

Krypton LEDs were attached to one steel faceplate per wall to measure its in-plane and out-of-plane displacements. Rosette strain gauges were installed at three levels on the other faceplate to directly measure strains at discrete locations. The locations of the LEDs and strain gauges on SC3 are presented in Fig. 5. The lateral load applied to each wall was calculated as the sum of the in-plane components of the actuator forces.

Experimental Results

Key test results are provided in Table 2. The initial stiffness of the SC walls, calculated at drift angles less than 0.02%, are presented in the second column of the table. The values of the forces and displacements corresponding to the onset of faceplate buckling are listed in the third and fourth columns, respectively. The fifth and sixth columns in the table present computed data at the onset of faceplate yielding, where forces and displacements were calculated using rosette strain gauge data and assuming a von Mises yield criterion. The seventh and eighth columns present peak loads and the corresponding drift angles for both EL+ and WL− directions. The last column in the table lists the postpeak loads corresponding to 3.3% drift angle, where tests were terminated, for both EL+ and WL− directions.

The initial stiffness of SC3 and SC4 was less than that of the thicker SC1. The initial stiffness of SC2 was also substantially less than SC1, which was not expected and is attributed to flexibility at

Table 2. Results Summary for SC1 through SC4

		Data point						
		Onset of steel plate buckling		Onset of steel plate yielding		Peak load		Test termination at 3.3% drift angle
						Load [kN (kips)]	Drift angle (%)	Load [kN (kips)]
Specimen	Initial stiffness [kN/mm (kips/in.)]	Load [kN (kips)]	Drift angle (%)	Load [kN (kips)]	Drift angle (%)	WL + /EL−	WL + /EL−	WL + /EL−
SC1	294 (1,680)	1,090 (245)	0.48	1,068 (240)	0.48	1,410/1,423 (317/320)	1.18/1.18	578/640 (130/144)
SC2	217 (1,240)	890 (200)	0.48	890 (200)	0.48	1,397/1,419 (314/319)	1.18/1.18	596/560 (134/126)
SC3	242 (1,380)	1,068 (240)	0.70	823 (185)	0.48	1,179/1,223 (265/275)	1.40/1.18	498/560 (112/126)
SC4	229 (1,310)	1,068 (240)	0.70	890 (200)	0.48	1,200/1,223 (270/275)	1.18/1.18	533/628 (120/141)

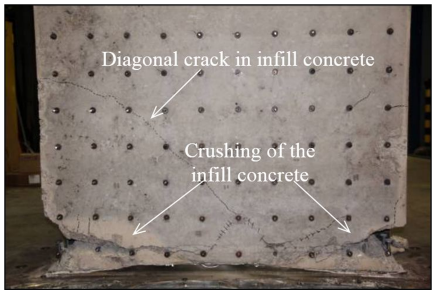

(a)

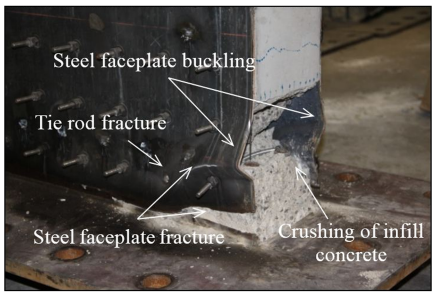

(b)

Fig. 6. Damage to SC2 at 3.3% drift angle: (a) infill concrete; (b) SC wall

the base of the wall. The faceplates buckled at their vertical free edges prior to achieving peak load. (Studs were not provided at the vertical free edges of the faceplates; see Fig. 1.) Plate buckling propagated towards the center of the wall during subsequent cycles of loading.

Yielding of the faceplates occurred prior to peak load. Peak load was observed at a drift angle of 1.1+%. The peak loads developed in SC1 and SC2, and in SC3 and SC4, are similar, which indicates that connector spacing in the range provided did not impact the peak shearing resistance in these flexure-critical walls. The peak loads in SC1 and SC2 are greater than SC3 and SC4 because the infill concrete is 76 mm (3 in.) thicker in SC1 and SC2.

Damage to SC Walls

Fig. 6 provides photographs of damage to SC2 at the end of the test. The progression of damage in the four SC walls was identical, sequentially (1) tensile cracking of the concrete at both ends of the wall, (2) outward buckling and yielding of the steel faceplates at the base of the wall, (3) crushing and spalling of concrete at the toes of the wall, and (4) tearing of the steel faceplates along their welded connection to the base plate.

A steel faceplate was removed from each of two specimens, SC2 and SC4, for the purpose of documenting damage to the infill concrete. As seen in Fig. 6(a), one wide diagonal crack formed in the infill concrete and most of the damage to the infill was concentrated immediately above the base plate, at the level of the first row of tie rods. No signs of splitting were observed in infill concrete.

Postpeak Response of SC Walls

Inelastic behavior of the four SC walls was associated with yielding of the steel faceplates near the base of the walls and damage to the infill concrete at the ends of the walls. Local buckling of the steel faceplates in the region of high plastic strain near the base of the walls triggered plate fracture and tearing.

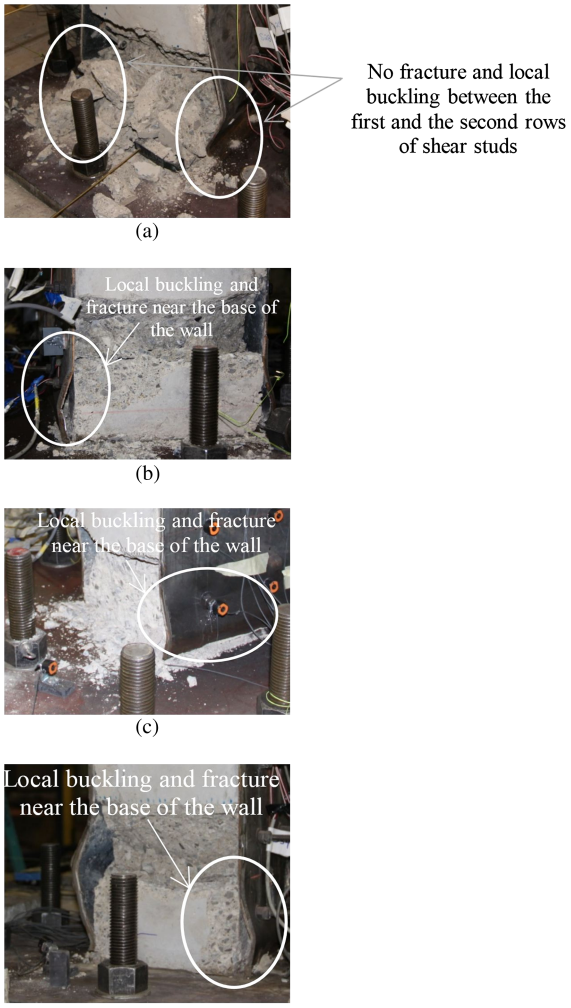

Fig. 7. Damage to the SC walls at 1.6% drift angle: (a) SC1; (b) SC2; (c) SC3; (d) SC4

Fig. 7 provides photographs of damage to the four walls at load step 10 (Fig. 4), which corresponds to a drift angle of 1.6%. The connectors in the first row were attached to the steel faceplates 51 mm (2 in.) (SC1) and 76 mm (3 in.) (SC2, SC3, and SC4) above

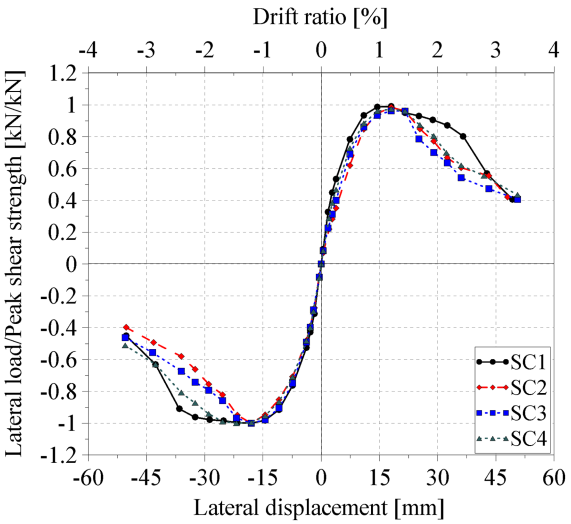

Fig. 8. Cyclic backbone curves for the SC walls

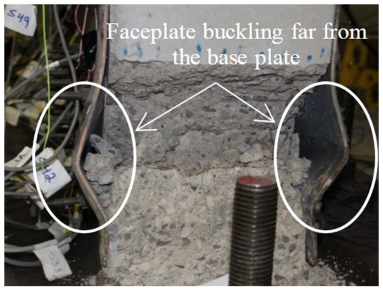

(a)

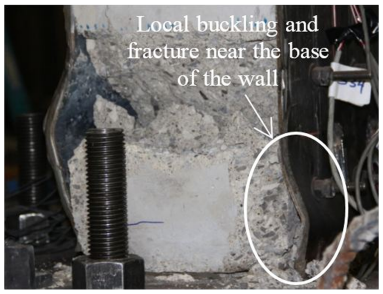

(b)

Fig. 9. Damage to SC4 at 1.6% drift angle: (a) west toe of the SC wall; (b) east toe of the SC wall

the welded connection of the faceplates to the baseplate. As seen in Fig. 7, local buckling of steel faceplates occurred above the first row of the connectors in SC1 and below the first row of connectors in SC2, SC3, and SC4. The use of a smaller distance [51 mm (2 in.)] between the baseplate and the first row of connectors in SC1 delayed the tearing of the faceplates and improved the postpeak response by forcing the inelastic buckling of the faceplates away from the CJP welded connection of the faceplates to the baseplate and into the panels defined by the first and second row of connectors.

The cyclic backbone curves of Fig. 8 provide further insight into the influence of the distance between the first row of the connectors and the base of the wall on the postpeak response of SC walls. The rate of the postpeak strength deterioration of SC1 is much less than other specimens, which is due to the fracture of the steel faceplates in SC2, SC3, and SC4 at a lower drift angle than in SC1. In SC4, the rate is slower in the EL− direction than in the WL+ direction because the steel faceplate buckled and fractured first at the east toe of the wall. Unexpectedly, the faceplate buckled far from the baseplate in the west toe of the SC4 (Fig. 9). The rate of the strength deterioration in SC2 and SC3 is almost identical in the EL− and WL+ directions.

Load-Displacement Cyclic Response

The load-displacement relationships for SC1 through SC4 are presented in Fig. 10. The load-displacement relationships are similar, with higher peak loads in the two thicker walls: SC1 and SC2. Prior to the yielding of the steel faceplates (drift angle of 0.48%; see Table 2) the residual drift ratios were less than 0.08%. The intracycle reduction of stiffness was observed first at displacements greater than those associated with yielding of the steel faceplates. Pinched hysteresis and loss of the strength and stiffness were observed for all walls, but occurred at displacements greater than those corresponding to peak strength. The pinching and strength degradation are attributed to faceplate buckling, cracking and crushing of the infill concrete, and tearing of the steel faceplate immediately above the baseplate.

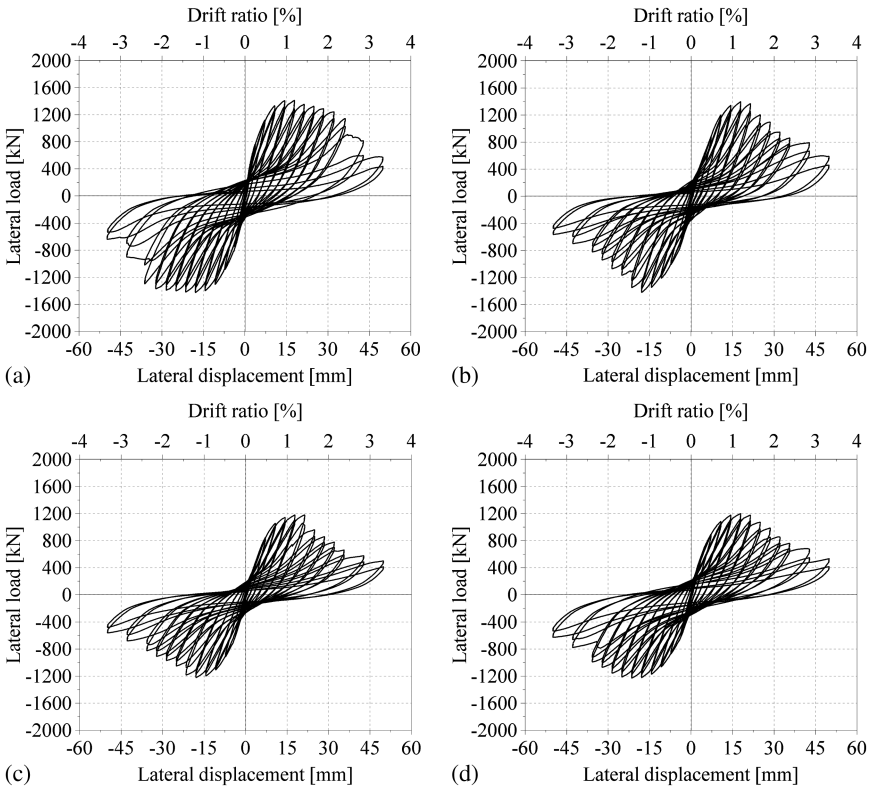

Fig. 10. Lateral load-displacement relationships of SC walls: (a) SC1; (b) SC2; (c) SC3; (d) SC4

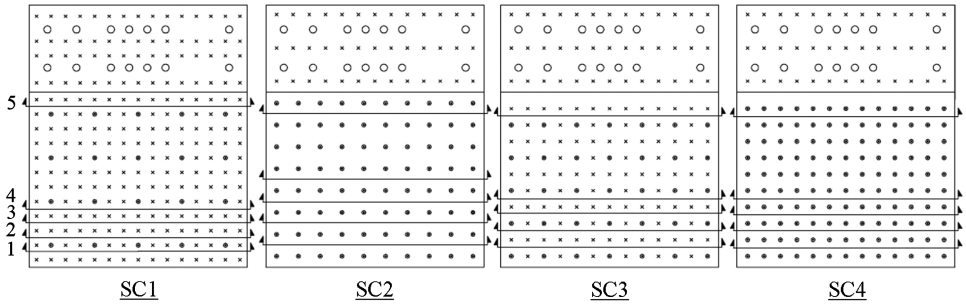

Fig. 11. Reporting levels for steel faceplates

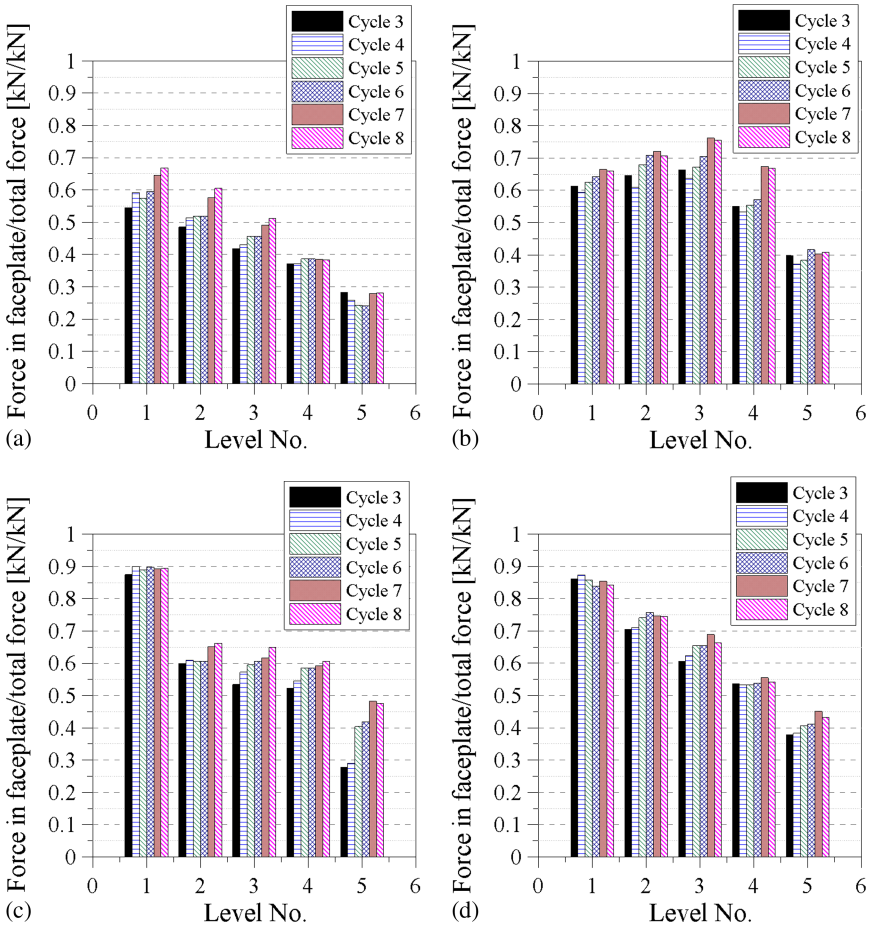

Fig. 12. Ratio of the horizontal shearing force resisted by the steel faceplates to the total applied load: (a) SC1; (b) SC2; (c) SC3; (d) SC4

Load Transfer in SC Walls

To investigate load transfer between the steel faceplate and the infill concrete, the strain field in the steel faceplates and horizontal shearing force resisted by the steel faceplates in the SC walls were evaluated at different elevations along the height of the wall using nodal displacements measured by the LEDs.

The square grid of Krypton LEDs installed on one faceplate per wall enabled calculation of the strain field in the elastic range of response. The horizontal and vertical displacements of the LEDs were used to calculate the three in-plane strain components using an isoparametric quadrilateral formulation [e.g., Bathe (1982)]. The normal and shear stresses were then calculated using an elastic constitutive stress-strain relationship. The horizontal shearing force resisted by the steel faceplates was calculated by integrating the shear stress along the length of the faceplates.

The horizontal shearing forces resisted by the steel faceplates were calculated at five levels along the height of the wall identified in Fig. 11. Fig. 12 presents results for cycles 3 through 8 and prior to faceplate yielding.

A force ratio is defined as the horizontal shearing force resisted by the steel faceplates divided by the total applied lateral force. The force ratio varies from 25 to 75% and from 30 to 90% for SC1/SC2 and SC3/SC4, respectively. The force ratios in SC3 and SC4 are greater than those in SC1 and SC3, supporting the intuitive statement that the higher the reinforcement ratio, the greater the steel faceplate contribution to the total shearing force.

The force ratios increase in SC1, SC3, and SC4 from the top of each specimen (level 5; see Fig. 11) to the foundation. The shearing force is transferred from the infill concrete to the steel faceplates through the connectors and interface friction between the infill

Table 3. Values of Measured and Predicted Stiffness for SC1 through SC4

Specimen	Measured initial stiffness [kN/mm (kips/in.)]	ABAQUS predictions	
		Rigid base [kN/mm (kips/in.)]	Flexible base [kN/mm (kips/in.)]
SC1	294 (1,680)	755 (4,310)	271 (1,550)
SC2	217 (1,240)	753 (4,300)	263 (1,500)
SC3	242 (1,380)	730 (4,170)	221 (1,260)
SC4	229 (1,310)	718 (4,100)	243 (1,390)

concrete and steel faceplate, along the height of the wall. In SC2, the specimen with the highest plate slenderness ratio (= 32), the greatest contribution of the steel faceplate to the total shearing force before yielding of the faceplate, is observed at level 3: the mid-height of the specimen. Ongoing numerical studies are investigating this issue.

The total horizontal shearing force transferred by a row of connectors was calculated as the difference between the horizontal shearing forces resisted by the steel faceplate above and below the row, which neglects interface friction. The shearing forces resisted by the second, third, and fourth rows of the connectors were estimated to be 49/62/89 kN (11/14/20 kips), 31/27/58 kN (7/6/13 kips), 120/18/22 kN (27/4/5 kips), and 58/45/72 kN (13/10/16 kips) for SC1 through SC4, respectively, in cycles 2 through 8 of Fig. 4. The shearing strengths of one anchor are 19 kN (4.3 kips) and 74 kN (16.5 kips) for steel failure and concrete pryout, respectively, per Appendix D of ACI 318-11 (ACI 2011). Setting aside the vertical shearing forces on the studs, the minimum nominal shearing strength of a row of connectors is 290/191/250/250 kN (65/43/56/56 kips), in SC1 through SC4, respectively, suggesting some margin against stud failure. No concrete crushing was observed around the tie rods in SC2 and SC4, which is not surprising given the calculated capacity of 74 kN (16.5 kips) per stud for concrete pryout.

Initial Stiffness

Initial stiffness is an important parameter for the analysis of structural systems incorporating SC walls. The measured and predicted values of initial stiffness for all tested SC walls are presented in Table 3. The measured initial stiffness of the SC walls was calculated at a drift angle of 0.02%. To investigate the effect of foundation flexibility due to the use of baseplate connection between the SC wall and the foundation block, two sets of ABAQUS models of the SC walls were prepared and analyzed: (1) including all components of the base connection and foundation block, and (2) assuming a rigid connection of the walls to an infinitely stiff base. The ABAQUS predictions of initial stiffness accounting for foundation flexibility recover the measured values very well. The assumption of a rigid base, which would be commonly made by practitioners, would lead to a substantial overestimation of initial stiffness.

Conclusions

Four large-scale rectangular SC walls (SC1 through SC4) were constructed at the Bowen Laboratory at Purdue University and the NEES facility at the University at Buffalo as part of a NSF-funded NEES project on low aspect ratio conventional and composite shear walls. The flexure-critical walls had an aspect ratio of 1.0. The walls were tested under reversed cyclic loading. The design space for the walls included the reinforcement ratio and faceplate slenderness ratio. A posttensioned bolted baseplate to the RC foundation connection was used for all four walls.

The key conclusions of the study reported herein are

1. The four walls sustained peak loads close to that predicted by pretest calculations using commercially available software. The faceplate slenderness ratio did not influence the peak resistance of the walls for the range of slenderness ratio studied (21–32);
2. The damage progression in the four walls was similar, namely, cracking and crushing of infill concrete at the toes of the walls, outward buckling and yielding of the steel faceplates near the base of the wall, and tearing of the faceplates at their junction with the base plate;
3. Pinched hysteresis and loss of stiffness and strength was observed in all four walls at lateral displacements greater than that corresponding to peak load. The rate of strength deterioration is affected by the faceplate slenderness ratio, with slightly better performance observed for values of the ratio less than the limit [Eq. (1)] proposed in the draft appendix to AISC N690s1;
4. The damage to the infill concrete was concentrated around the level of the first row of connectors in all four walls;
5. The distance between the first row of the connectors and the base of the wall has a significant influence on the postpeak load behavior of these types of SC walls. The use of a smaller distance between the first row of connectors and the baseplate in SC1 resulted in slower postpeak strength deterioration in SC1 than in SC2 through SC4;
6. At the foundation level, lateral load is resisted primarily by the steel faceplates: at peak load, the steel faceplates resisted more than 75% of the total shearing force; and
7. Numerical studies of the initial stiffness of the SC walls show the importance of addressing the flexibility caused by posttensioning an SC wall to its foundation. Foundation flexibility should be modeled when calculating demands on structures, systems, and components.

Acknowledgments

This project was supported in part by the U.S. National Science Foundation under Grant No. CMMI-0829978. This support is gratefully acknowledged. We thank the technical staff of the NEES laboratory at the University of Buffalo, and the Bowen Laboratory at Purdue University, and LPCiminelli Inc. for their contributions to the project.

References

ACI Committee 318. (2011). "Building code requirements for structural concrete and commentary." *ACI 318-11*, American Concrete Institute, Farmington Hills, MI.

ACI Committee 374.1. (2005). *Acceptance criteria for moment frames based on structural testing and commentary*, American Concrete Institute, Farmington Hills, MI.

Adams, P. F., Zimmerman, T. J. E., and MacGregor, J. G. (1987). "Design and behaviour of composite ice-resisting walls." *Proc., 9th Int. Conf. on Port and Ocean Engineering under Arctic Conditions*, Univ. of Alaska, Fairbanks, AK, 663–674.

Akita, S., Ozaki, M., Niwa, N., Matsuo, I., and Hara, K. (2001). "Study on steel plate reinforced concrete bearing wall for nuclear power plants (part #2). analytical method to evaluate response of SC walls." *Trans., 16th Int. Conf. on Structural Mechanics in Reactor Technology (SMiRT16)*, International Association for Structural Mechanics in Reactor Technology (IASMiRT), North Carolina State Univ., Raleigh, NC.

Akiyama, H., Sekimoto, H., Tanaka, M., Inoue, K., Fukihara, M., and Okuda, Y. (1989). "1/10th scale model test of inner concrete structure composed of concrete filled steel bearing wall." *Trans., 10th Int. Conf. on Structural Mechanics in Reactor Technology (SMiRT10)*, International Association for Structural Mechanics in Reactor Technology (IASMiRT), North Carolina State Univ., Raleigh, NC.

American Institute of Steel Construction (AISC). (2014). "Specification for safety-related steel structures for nuclear facilities, supplement No. 1." *N690s1*, Chicago, IL.

Bathe, K. (1982). *Finite element procedures in engineering analysis*, Prentice Hall, Englewood Cliffs, NJ.

Booth, P. N., Varma, A. H., Malushte, S. R., and Johnson, W. H. (2007). "Response of modular composite walls to combined thermal & mechanical load." *Trans., 19th Int. Conf. on Structural Mechanics in Reactor Technology (SMiRT19)*, Toronto.

Chadwell, C. B., and Imbsen, R. A. (2002). "XTRACT-cross section analysis software for structural and earthquake engineering." TRC, Rancho Cordova, CA, ⟨http://www.imbsen.com/xtract.htm⟩ (Aug. 30, 2011).

Epackachi, S. (2014). "Analytical, numerical, and experimental studies on steel-concrete composite walls." Ph.D. dissertation, Dept. of Civil, Structural and Environmental Engineering, Univ. at Buffalo, Buffalo, NY.

Gerwick, B. C., and Dale, B. (1987). "Utilization of composite design in the arctic and sub-arctic." *Proc., 9th Int. Conf. on Port and Ocean Engineering under Arctic Conditions*, Univ. of Alaska, Fairbanks, AK, 655–662.

JEA. (2005). "Technical guidelines for seismic design of steel plate reinforced concrete structures: Buildings and structures." *JEAG 4618*, Japanese Electric Association, Tokyo.

Kazuaki, T., et al. (2001). "Experimental study on steel plate reinforced concrete shear walls with joint bars." *Trans. 16th Int. Conf. on Structural Mechanics in Reactor Technology (SMiRT16)*, Washington, DC.

Link, R. A., and Elwi, A. E. (1995). "Composite concrete-steel plate walls: Analysis and behavior." *J. Struct. Eng.*, 10.1061/(ASCE)0733-9445(1995)121:2(260), 260–271.

Matsuishi, M., and Iwata, S. (1987). "Strength of composite, sandwich system, ice-resisting structures." *Proc., 9th Int. Conf. on Port and Ocean Engineering under Arctic Conditions*, Univ. of Alaska, Fairbanks, AK, 689–698.

Oduyemi, T. O. S., and Wright, H. D. (1989). "Experimental investigation into the behaviour of double-skin sandwich beams." *J. Constr. Steel Res.*, 14(3), 197–220.

O'Flynn, B., and MacGregor, J. G. (1987). "Tests on composite ice-resisting walls." *Proc., 9th Int. Conf. on Port and Ocean Engineering under Arctic Conditions*, Univ. of Alaska, Fairbanks, AK, 699–710.

Ozaki, M., Akita, S., Niwa, N., Matsuo, I., and Usami, S. (2001). "Study on steel plate reinforced concrete bearing wall for nuclear power plants (part #1). Shear and bending loading tests of SC walls." *Trans., 16th Int. Conf. on Structural Mechanics in Reactor Technology (SMiRT16)*, International Association for Structural Mechanics in Reactor Technology (IASMiRT), North Carolina State Univ., Raleigh, NC.

Ozaki, M., Akita, S., Osuga, H., Nakayama, T., and Adachi, N. (2004). "Study on steel plate reinforced concrete panels subjected to cyclic in-plane shear." *Nucl. Eng. Des.*, 228(1–3), 225–244.

Sasaki, N., Akiyama, H., Narikawa, M., Hara, K., Takeuchi, M., and Usami, S. (1995). "Study on a concrete filled steel structure for nuclear power plants (part #3). Shear and bending loading tests on wall member." *Trans., 13th Int. Conf. on Structural Mechanics in Reactor Technology (SMiRT13)*, International Association for Structural Mechanics in Reactor Technology (IASMiRT), North Carolina State Univ., Raleigh, NC.

Sener, K., and Varma, A. H. (2014). "Steel-plate composite SC walls: Experimental database and design for out-of-plane shear." *J. Constr. Steel Res.*, 100, 197–210.

SIMULIA. (2012a). "Abaqus analysis user's manual." *Version 6.12*, Dassault Systèmes Simulia Corp., Providence, Rhode Island.

SIMULIA. (2012b). "Abaqus theory manual." *Version 6.12*, Dassault Systèmes Simulia Corp., Providence, Rhode Island.

Smith, J. R., and McLeish, A. (1987). "The resistance of composite steel/concrete structures to localized ise loading." *Proc., 9th Int. Conf. on Port and Ocean Engineering under Arctic Conditions*, Univ. of Alaska, Fairbanks, AK, 675–687.

Takeda, T., Yamaguchi, T., Nakayama, T., Akiyama, K., and Kato, Y. (1995). "Experimental study on shear characteristics of concrete filled steel plate wall." *Trans., 13th Int. Conf. on Structural Mechanics in Reactor Technology (SMiRT13)*, International Association for Structural Mechanics in Reactor Technology (IASMiRT), North Carolina State Univ., Raleigh, NC.

Takeuchi, M., Akiyama, H., Narikawa, M., Hara, K., Tsubota, H., and Matsuo, I. (1995). "Study on a concrete filled steel structure for nuclear power plants (part #1): Outline of the structure and the mock-up test." *Trans., 13th Int. Conf. on Structural Mechanics in Reactor Technology (SMiRT13)*, International Association for Structural Mechanics in Reactor Technology (IASMiRT), North Carolina State Univ., Raleigh, NC.

Usami, S., Akiyama, H., Narikawa, M., Hara, K., Takeuchi, M., and Sasaki, N. (1995). "Study on a concrete filled steel structure for nuclear power plants (part #2). Compressive loading tests on wall members." *Trans., 13th Int. Conf. on Structural Mechanics in Reactor Technology (SMiRT13)*, International Association for Structural Mechanics in Reactor Technology (IASMiRT), North Carolina State Univ., Raleigh, NC.

Varma, A. H., Malushte, S., Sener, K., and Lai, Z. (2014). "Steel-plate composite (SC) walls for safety related nuclear facilities: Design for in-plane force and out-of-plane moments." *Nucl. Eng. Des.*, 269, 240–249.

Varma, A. H., Malushte, S. R., Sener, K., and Booth, P. N. (2012). "Analysis recommendations for steel-composite walls for safety-related nuclear facilities." *Proc., ASCE Structures Congress*, ASCE, Reston, VA, 1871–1880.

Varma, A. H., Sener, K., and Mitsubishi Heavy Industries Ltd. (2013). "Lateral load behavior of a pressurized water reactor containment internal structure." *Trans., 22nd Int. Conf. on Structural Mechanics in Reactor Technology (SMiRT22)*, International Association for Structural Mechanics in Reactor Technology (IASMiRT), North Carolina State Univ., Raleigh, NC.

Varma, A. H., Zhang, K., Chi, H., Booth, P., and Baker, T. (2011). "In-plane shear behavior of SC composite walls: Theory vs. experiment." *Trans., 21st Int. Conf. on Structural Mechanics in Reactor Technology (SMiRT21)*, International Association for Structural Mechanics in Reactor Technology (IASMiRT), North Carolina State Univ., Raleigh, NC.

Wright, H. D., Oduyemi, T. O. S., and Evans, H. R. (1991a). "Design of double skin composite elements." *J. Constr. Steel Res.*, 19(2), 111–132.

Wright, H. D., Oduyemi, T. O. S., and Evans, H. R. (1991b). "The experimental behaviour of double skin composite elements." *J. Constr. Steel Res.*, 19(2), 97–110.

Zhang, K., Varma, A. H., Malushte, S., and Gallocher, S. (2014). "Effects of shear connectors on the local buckling and composite action in steel concrete composite walls." *Nucl. Eng. Des.*, 269, 231–239.